Improved susceptibility quantification with effective magnetic moment

S. Liu[1], J. Neelavalli[2], J. Tang[1], and E. M. Haacke[2,3]

[1]School of Biomedical Engineering, McMaster University, Hamilton, Ontario, Canada, [2]The Magnetic Resonance Imaging Institute for Biomedical Research, Detroit, Michigan, United States, [3]Academic Radiology, Wayne State University, Detroit, Michigan, United States

Introduction: Quantifying magnetic susceptibility of microbleeds is very important for studying and elucidating longitudinal changes in them in conditions like Traumatic Brain Injury (TBI), cerebral amyloid angiopathy, Alzheimer's, or even in dementia and normal aging [1]. In most newly developed methods, susceptibility quantification is usually done by solving an inverse problem, which is based on the simple relation between susceptibility distribution and magnetic field perturbation in Fourier domain [2-4]. The accuracy of all of these methods, however, is a function of the apparent phase and volume of the object, in the phase and magnitude MR images from the gradient echo sequence. Signal loss due to T_2* effects causes an increase in the apparent volume of a given microbleed. To minimize this, a short echo time (TE) gradient echo sequence could be used. However, susceptibility quantification is predicated on phase information and requires sufficiently long TEs to obtain high phase-SNR. But, T_2* effects also increase with increasing TE. Essentially, since the object susceptibility and volume are in product relation, one cannot tease out the true susceptibility of the object without the knowledge of the true object volume. If an estimate of the true volume of the microbleed is known from a spin-echo dataset (which is free of T_2* effects), it may be possible to obtain their actual susceptibility value using the magnetic moment measurements from the gradient echo data. To evaluate this, we carried out a gel phantom study with air bubbles mimicking the microbleeds.

Materials and Methods: For a sphere with a susceptibility difference of $\Delta\chi$ with its surroundings, the magnetic field perturbation outside the sphere can be described as $\Delta B_{out}(r)= \Delta\chi a^3(3\cos^2\theta-1)B_0/(3r^3)$[5]. The product of $\Delta\chi a^3$, i.e. the magnetic moment, is constant for a given B_0. In gradient echo imaging, the apparent volume of the air-bubble increases due to additional T_2' dephasing which in turn is due to the field perturbation profile outside. Since susceptibility mapping process only deconvolves the dipolar phase, irrespective of the true volume of the object, the deconvolved susceptibility value is $\Delta\chi'$ corresponding to an increased apparent volume V'. However, theoretically, $\Delta\chi'V'=\Delta\chi V$ (*Eqn.1*). Given an estimate of the true volume, V from a Spin echo sequence, using Eqn.1, one could obtain $\Delta\chi$ value accurately. This hypothesis was tested on a gel phantom containing small air-bubbles. The theoretical susceptibility difference between gel and air is known to be 9ppm and air bubbles can be well approximated as spheres. Agarose gel solution was prepared at 8% concentration by weight and poured into a cylindrical container. Variable sized bubbles were obtained using air pumped from an empty syringe. The phantom was imaged at 3T (Siemens Verio) using two multi-echo (4 echoes each) gradient echo sequences. The TEs in the first sequence are 3.25ms, 5.52ms, 7.79ms, 10.06ms, and the TEs in the second sequence are 4.25ms, 6.52ms, 8.79ms, and 11.06ms. Other parameters are as follows: TR 15ms, FA 12º, BW 543 Hz/pixel, voxel size 0.6x0.6x0.6mm^3, and matrix size 512x512x128. A Spin Echo dataset was collected with FA 90 º, TR 5000ms, TE 14ms. All the other parameters are the same between gradient echo and spin echo acquisitions. The mean and standard deviation of the susceptibility values inside the bubble were measured from the susceptibility maps [2]; while the volume was measured from magnitude images, in a way similar to the "Object Strength" proposed by Tofts et al[6]. Phase images were first unwrapped and background field effects were removed using the forward field estimation method [7].

Results: The susceptibility and volume were measured for 14 bubbles at 8 different TEs. The ratios between the magnetic moments measured at every two different TEs are calculated for each bubble ($\Delta\chi_1'V_1'$ at lower TE /$\Delta\chi_2'V_2'$ at higher TE; total 28 pair ratios for a single air-bubble) and the histogram of these ratios is shown in Fig 1.A. As expected, this distribution is centered around 1, indicating the magnetic moments are generally the same at different TEs for the same bubble. Normalized volumes (normalized to volume at shortest TE) measured for 3 bubbles at different TEs are plotted in Fig 1B; clearly showing a linear trend in volume increase with TE. The susceptibility of the air bubbles at different TEs was measured to be 1.4 ppm/0.6ppm (mean/standard deviation). Using the volume measured in the Spin Echo dataset, the susceptibility of the air bubbles was corrected to 6.2ppm/1.6ppm (mean/standard deviation). The volumes of the 14 bubbles measured from the Spin Echo dataset range from 2.7 voxels to 27.1 voxels, with a median volume of 6.3 voxels. Figure 1.C shows the histogram of susceptibility distribution of the air-bubbles at different TEs, and Fig 1.D shows the corresponding distribution for 'corrected' susceptibility values obtained using Eqn. 1. A clear shift in the susceptibility value distribution is seen.

Discussions and Conclusions: The susceptibilities of those air bubbles are severely under-estimated using the original susceptibility mapping method. This is mainly due to the apparent volume of the bubble which is larger than the true volume by about a factor of 2. As expected, the effective magnetic moment generally stays as a constant at different TEs. The true volume was estimated from a spin echo dataset in this study. When corrected using the volume estimated from spin-echo data, the susceptibility value estimates moved closer to the actual susceptibility value of 9ppm. Generally, the error in susceptibility quantification dropped from 84% to 31%.

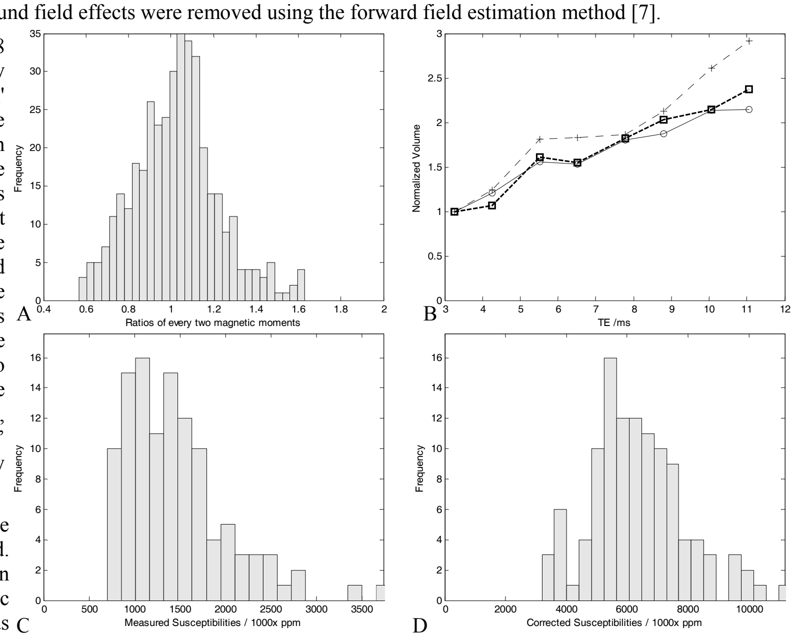

***FIG 1**: **(A)** Histogram of the ratio between the magnetic moments measured at every two different TEs for a given bubble. **(B)**Normalized volume of 3 air-bubbles measured at different TEs. **(C)** Histogram of the measured susceptibilities at different TEs. **(D)** Corresponding distribution of the corrected susceptibilities.*

The persistent underestimation for these small bubbles is mainly due to error in the estimated volume of these bubbles from the spin echo data. Although a regression based method was used for volume measurement [6], it is still influenced by partial voluming and Gibbs ringing in the magnitude images which introduces errors in the volume measurement. Furthermore, such errors in volume measurement from gradient echo data will also influence magnetic moment measures. Evidence of this is seen in the large spread in the histograms shown in Fig 1C and D and partly the spread in Fig 1A as well. Interestingly, when the volumes of the air-bubbles measured from gradient echo data as a function of TE were extrapolated to a TE=0, these zero-TE-intercept-volumes were very similar to those measured from the spin-echo data. This indicates that it may be possible to obtain true volume estimates from multi-echo gradient echo data itself which can obviate the need of spin echo acquisition. However, the zero-TE-intercept-volume is a function of the effective T2' decay around the bubble [8]. This will be the focus of our future work. Nonetheless, the fact that despite volume measurement from spin echo data, the actual susceptibility of the bubbles was not obtained for small air bubbles indicates the need for higher resolution imaging for better volume estimation. In conclusion, we have shown that for very small structures, obtaining accurate magnetic susceptibility values may be limited by the error in volume estimate of these structures.

References: [1]Ayaz M et al., JMRI(2010);31:142-8. [2] Haacke et al. JMRI(2010);32:663-76 [3] Kressler et al. IEEE Trans. Med. Imaging(2010);29:273-81 [4] Wharton et al. MRM(2010);63:1292-1304. [5] Haacke et al.(1999)MRI: Physical Principles and Sequence Design (Wiley). [6]Tofts et al. MAGMA(2005); 18(3): 162-9. [7] Neelavalli et al., JMRI(2009);29:938-48. [8] Cheng YC-N et al.,MRI(2001);19:1017-23.